Electronic supplementary information

Synergistic effects of Ni–Fe alloy catalysts on dry reforming of methane at low temperatures in electric field

Ayaka Motomura[a], Yuki Nakaya[b], Sampson Clarence[a], Takuma Higo[a], Maki Torimoto[a], Hideaki Tsuneki[a], Shinya Furukawa[b] and Yasushi Sekine[*a]

a. Department of Applied Chemistry, Waseda University, 3-4-1, Okubo, Shinjuku, Tokyo, 169-8555, Japan, *E-mail: ysekine@waseda.jp

b. Institute for Catalysts, Hokkaido University, Kita 21 Nishi 10, Kita-ku, Sapporo, 001-0021, Japan.

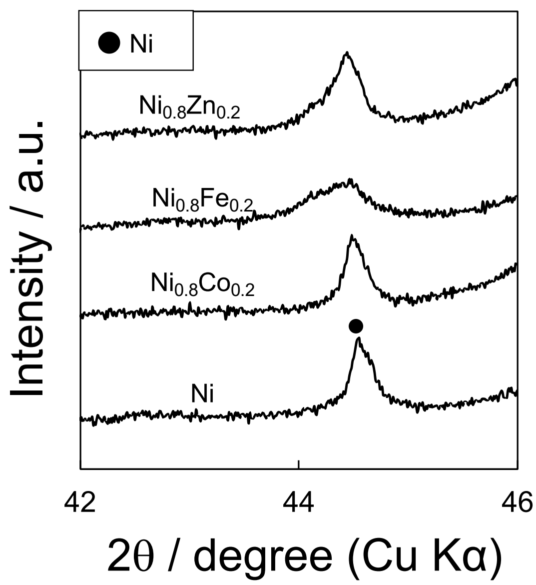

Figure S1 XRD patterns of 10wt%Ni, ($Ni_{0.8}M_{0.2}$) (M = Co, Fe, Zn) /CeO_2.

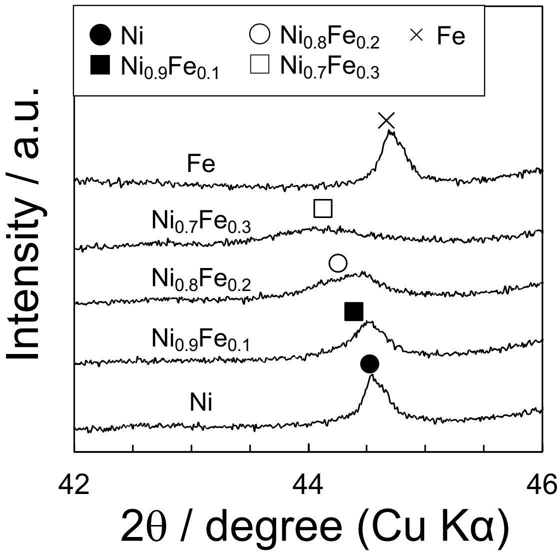

Figure S2 XRD patterns of 10wt%Ni, ($Ni_{1-x}M_x$) (X = 0.1, 0.2, 0.3 and only Fe) /CeO_2.

Experimental results

Table S1 Catalytic activity of 10wt%Ni, ($Ni_{0.8}M_{0.2}$) (M = Co, Zn), ($Ni_{1-x}Fe_x$) (x = 0.1, 0.2, 0.3)/CeO_2.

Table S1. Catalytic activities of DRM with or without EF

(a) At 673 K with/without EF for the reaction rate and H_2/CO ratio.

Catalyst	Without EF (673 K)			With EF (673 K, 10 mA)	
	Reaction rate of CH_4 / mmol h^{-1} g_{Ni}^{-1}	Amount of carbon deposition / g-C/g-cat.	H_2/CO	Reaction rate of CH_4 / mmol h^{-1} g_{Ni}^{-1}	H_2/CO
Ni	129.3	0.141	0.50	124.8	0.48
$Ni_{0.8}Co_{0.2}$	146.6	0.079	0.49	140.0	0.48
$Ni_{0.9}Fe_{0.1}$	109.5	0.173	0.49	103.5	0.51
$Ni_{0.8}Fe_{0.2}$	91.5	0.009	0.38	78.2	0.37
$Ni_{0.7}Fe_{0.3}$	14.2	0.006	0.17	14.1	0.17
$Ni_{0.8}Zn_{0.2}$	85.9	0.021	0.35	90.1	0.38

(b) At 473 K with/without EF for the reaction rate and H_2/CO ratio.

Catalyst	Without EF (473 K)		With EF (473 K, 10 mA)			
	Reaction rate of CH_4 / mmol h^{-1} g_{Ni}^{-1}	H_2/CO	Reaction rate of CH_4 / mmol h^{-1} g_{Ni}^{-1}	Activity/ kWh kg-syngas^{-1}	Amount of carbon deposition / g-C/g-cat.	H_2/CO
Ni	0.1	0	20.8	1.94	0.035	0.74
$Ni_{0.8}Co_{0.2}$	0.2	0	54.8	1.71	0.024	0.77
$Ni_{0.9}Fe_{0.1}$	0.3	0	112.2	1.67	0.021	0.81
$Ni_{0.8}Fe_{0.2}$	0.4	0	174.4	1.43	0.015	0.82
$Ni_{0.7}Fe_{0.3}$	0.6	0	0.1	29.0	0.006	0.13
$Ni_{0.8}Zn_{0.2}$	0.3	0	77.7	1.42	0.022	0.75

(c) At 673 K with/without EF for the conversion and yield.

Catalyst	Without EF (673 K)				With EF (673 K, 10 mA)			
	CH_4 conversion / %	CO_2 conversion / %	H_2 yield/ %	CO yield/ %	CH_4 conversion/ %	CO_2 conversion / %	H_2 yield/ %	CO yield/ %
Ni	4.8	7.7	3.2	4.8	4.9	8.0	3.2	4.9
$Ni_{0.8}Co_{0.2}$	4.9	7.7	3.3	4.9	4.8	7.8	3.1	4.8
$Ni_{0.9}Fe_{0.1}$	4.6	7.0	3.0	4.6	4.3	6.7	2.9	4.3
$Ni_{0.8}Fe_{0.2}$	3.0	5.6	1.6	3.0	2.6	5.0	1.3	2.6
$Ni_{0.7}Fe_{0.3}$	0.4	1.1	0.1	0.4	0.4	1.1	0.1	0.4
$Ni_{0.8}Zn_{0.2}$	2.9	5.7	1.5	2.9	3.1	5.7	1.7	3.1

(d) At 673 K with/without EF for the conversion and yield.

Catalyst	Without EF (473 K)				With EF (473 K, 10 mA)			
	CH_4 conversion / %	CO_2 conversion / %	H_2 yield/ %	CO yield/ %	CH_4 conversion / %	CO_2 conversion / %	H_2 yield/ %	CO yield/ %
Ni	0.0	0.0	0.0	0.0	0.8	1.2	0.7	0.8
$Ni_{0.8}Co_{0.2}$	0.0	0.0	0.0	0.0	1.9	2.5	1.6	1.9
$Ni_{0.9}Fe_{0.1}$	0.0	0.0	0.0	0.0	4.3	5.1	3.9	4.3
$Ni_{0.8}Fe_{0.2}$	0.0	0.0	0.0	0.0	6.0	6.5	5.7	6.0
$Ni_{0.7}Fe_{0.3}$	0.0	0.1	0.0	0.0	0.0	0.0	0.0	0.0
$Ni_{0.8}Zn_{0.2}$	0.0	0.0	0.0	0.0	4.9	7.7	2.1	4.9

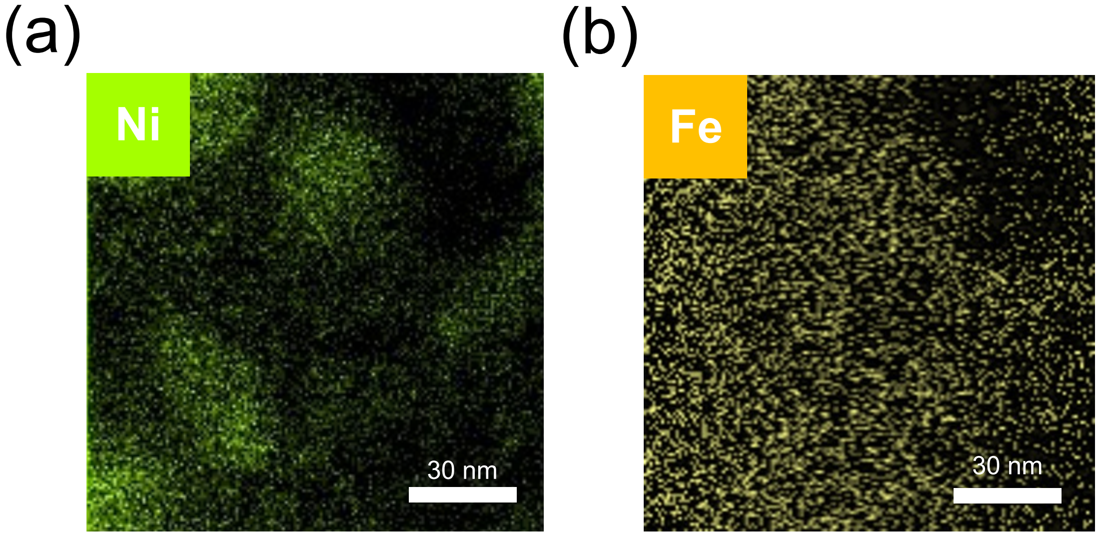

Figure S3 EDX mappings for 10wt%($Ni_{0.7}Fe_{0.3}$)/CeO_2.

Evaluation of adsorbed species on Ni, $Ni_{0.8}Fe_{0.2}$ /CeO_2

Figure S4 shows H_2-TPD patterns of Ni, $Ni_{0.8}Fe_{0.2}$/CeO_2 extracted from H_2 mass signal. Temperature of H_2 desorption on $Ni_{0.8}Fe_{0.2}$ shifted to the lower side by about 40 K rather than that of Ni. The desorption peak at temperatures among lower than 573 K is attributed to H_2 desorbed from the surface Ni particles.[a, b] This result demonstrates that $Ni_{0.8}Fe_{0.2}$ has lower H_2 adsorption ability and weaker interaction of adsorbed H atoms than Ni–monometallic. In EF-assisted catalytic reaction, H atom adsorption energy effects on the surface proton migration and thus reactivity. Also, proper adsorption energy is required for high mobility and activity.[c] In view of this report, $Ni_{0.8}Fe_{0.2}$ which shows high activity with EF is expected to have appropriate H atom adsorption ability and allow protons to migrate easily for achieving high catalytic activity.

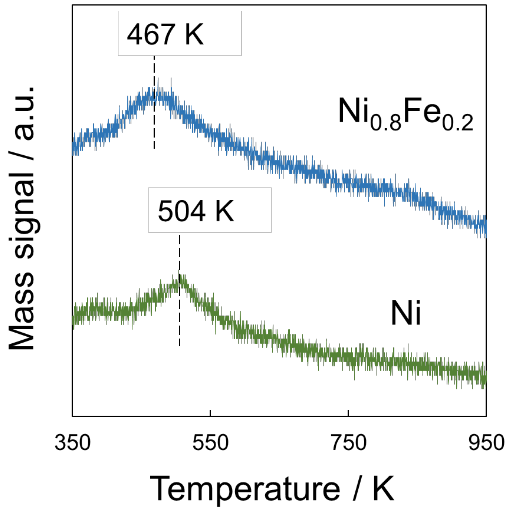

Figure S4 H_2-TPD patterns of 10wt%Ni, $(Ni_{0.8}Fe_{0.2})/CeO_2$.

Also, the number of adsorbed species is already known to play an important role in proton conduction *via* hydroxyl groups on the catalyst surface.[24, d] Because adsorbed species such as surface hydroxyl groups can be stable at low temperatures, EF application is the predominant result at the low temperature side. Contrary, at high temperatures, the effect of EF application is reduced, and the heat catalytic reaction becomes dominant because the adsorbed species are desorbed. Temperature variation tests using Ni, $Ni_{0.8}Fe_{0.2}/CeO_2$ were conducted to investigate the effects of temperature on activity and adsorbed species (results are depicted in Figures S5).

Although the temperature is reduced, the adsorbed species, which are carriers of proton conduction, do not desorb. Because the adsorption phenomenon is an exothermic reaction, the adsorbed species desorb gradually as the temperature is increased. Consequently, the influence of the state of the adsorbed species on the activity is visible from the temperature change test: for Ni, the processes of lowering and raising the catalyst bed temperature showed different behaviours. In the process of lowering the temperature, the activity decreased gradually, concomitantly with decreasing temperature. In the process of increasing the temperature from 373 K, the activity decreased significantly with increasing temperature. However, $Ni_{0.8}Fe_{0.2}$ showed an almost identical trend at lower and higher temperatures. At temperatures higher than

473 K, the adsorbed species start to desorb, resulting in a marked decrease in activity and higher temperature dependence.

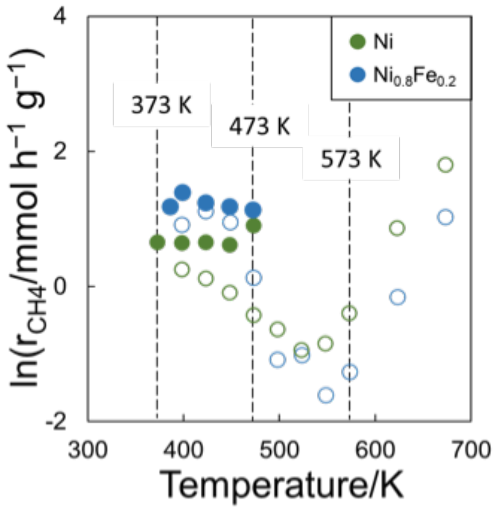

Figure S5 Relationship between temperature and activity of 10wt%Ni, 10wt%($Ni_{0.8}Fe_{0.2}$)/CeO_2 with application of 5 mA; 80 SCCM total flow rate (CH_4: CO_2: Ar = 1: 1: 6); open symbols represent the data with ramping temperatures, closed symbols represent the data with decreasing temperatures.

a) Z. Luo, Z. Zheng, L. Li, Y. Cui and C. Zhao, *ACS catal.*, 2017, 7, 8304-8313.

b) S. Velu and S. K. Gangwal, *Solid State Ion.*, 2006, 177, 803-811.

c) K. Murakami, Y. Mizutani, H. Sampei, A. Ishikawa, Y. Tanaka, S. Hayashi, S. Doi, T. Higo, H. Tsuneki, H. Nakai and Y. Sekine, *Phys. Chem. Chem. Phys.,* 2021, 23, 4509-4516.

d) A. Takahashi, R. Inagaki, M. Torimoto, Y. Hisai, T. Matsuda, Q. Ma, J. G. Seo, T. Higo, H. Tsuneki, S. Ogo, T. Norby and Y. Sekine, *RSC Adv.,* 2020, 10, 14487-14492.